British Journal of Pharmacology (2004) 142, 1002–1014
www.nature.com/bjp

Methylene ATP analogs as modulators of extracellular ATP metabolism and accumulation

[1]Sheldon M. Joseph, [1]Matthew A. Pifer, [2]Ronald J. Przybylski & *,[1]George R. Dubyak

[1]Department of Physiology and Biophysics, E565, School of Medicine, Case Western Reserve University, Cleveland, OH 44106, U.S.A. and [2]Department of Anatomy, E565, School of Medicine, Case Western Reserve University, Cleveland, OH 44106, U.S.A.

1 Transient accumulation of extracellular ATP reflects both release of ATP from intracellular stores and altered rates of ATP metabolism by ecto-enzymes. Ecto-nucleoside triphosphate diphosphohydrolases (eNTPDases) and ecto-nucleotide pyrophosphatases (eNPPs) degrade ATP, while ecto-nucleotide diphosphokinases (eNDPKs) synthesize ATP from ambient ADP.

2 Although the methylene ATP analogs $\beta\gamma$-meATP and $\alpha\beta$-meATP are widely used as metabolically stable tools for the analysis of purinergic signaling, their specific effects on eNTPDase, eNPP, and eNDPK activities have not been defined. This study compared the actions of these analogs on extracellular ATP metabolism by human 1321N1 astrocytes, rat PC12 pheochomocytoma cells, and rat C6 glioma cells.

3 Both analogs significantly reduced clearance of extracellular ATP by 1321N1 cells that express both eNTPDases and eNPPs, as well as by C6 cells that exclusively express eNPPs. In contrast, both analogs were much less efficacious in inhibiting ATP clearance by PC12 cells that predominantly express eNTPDases. $\beta\gamma$-meATP, but not $\alpha\beta$-meATP, was effectively hydrolyzed by the 1321N1 and C6 cells; PC12 cells did not significantly degrade this analog.

4 $\alpha\beta$-meATP, but not $\beta\gamma$-meATP, acted as a substrate for purified yeast NDPK to generate ATP *via trans*-phosphorylation of ADP. $\alpha\beta$-meATP also acted as substrate for the eNDPK activities expressed by 1321N1, PC12, and C6 cells and thereby induced extracellular ATP accumulation in the presence of ambient or exogenously added ADP.

5 These results indicate that methylene ATP analogs exert complex and cell-specific effects on extracellular ATP metabolism that can significantly modify interpretation of studies that use these reagents as probes of purinergic signal transduction in intact tissues.
British Journal of Pharmacology (2004) **142,** 1002–1014. doi:10.1038/sj.bjp.0705865

Keywords: Extracellular ATP; ecto-ATPase; ecto-nucleoside triphosphate diphosphohydrolase; ecto-nucleotide pyrophosphatase/phosphodiesterase; β,γ-methylene ATP; α,β-methylene ATP; nucleotide diphosphokinase; astrocyte; pheochromocytoma; glioma

Abbreviations: ATP, adenosine-5′-triphosphate; $\alpha\beta$-meATP, α,β-methylene ATP; $\beta\gamma$-meATP, β,γ-methylene ATP; NS-AP, nonspecific alkaline phosphatase; eNPP, ecto-nucleotide pyrophosphatase/phophodiesterase; eNTPDase/CD39, ecto-nucleoside 5′-triphosphate diphosphohydrolase; εATP, etheno-adenosine-5′-triphosphate; GPI, glycosylphosphatidylinositol; NDPK, nucleotide diphosphokinase

Introduction

When present in extracellular compartments, adenosine-5′-triphosphate (ATP) and other nucleotides act as agonists for the P2 family of cell surface receptors. To date, eight members of the G protein-coupled P2Y receptor family and seven subtypes of the ionotropic P2X receptor family have been identified (Ralevic & Burnstock, 1998; North, 2002; Lazarowski *et al*., 2003a). Studies using pharmacological reagents or knockout mice that lack certain P2 nucleotide receptor subtypes have demonstrated important physiological roles for extracellular ATP or its metabolites in hemostasis, neuronal function, fertility, inflammation, and ion transport (Dunn, 2000; Foster *et al*., 2001; Gachet, 2001; Vlaskovska *et al*., 2001; Labasi *et al*., 2002; Robaye *et al*., 2003). As all cells contain ATP, most cell types are potential sources of extracellular ATP. ATP is released either constitutively or when cells are stimulated within tissue-specific physiological or pathophysiological contexts (Lazarowski *et al*., 2003a). The released ATP, or its metabolites, can then activate the various P2 receptors that are widely expressed in mammalian tissues.

The ability of ATP to act as an intercellular signaling molecule depends on the rate and extent of its accumulation in interstitial tissue spaces and cell–cell junctions. As extracellular ATP accumulation reflects changes in the rates of ATP release, hydrolysis by ecto-ATPases, and synthesis by ecto-nucleotide diphosphokinases (eNDPKs) (Lazarowski *et al*., 1997; 2000; Zimmermann, 2000; Yegutkin *et al*., 2001; 2002), analysis of the mechanisms by which mammalian cells release ATP into external spaces requires an understanding of the ecto-enzymes that regulate ATP metabolism within such compartments.

Four major families of ecto-nucleotidases have been identified (Zimmermann, 2000): (1) the ecto-nucleoside 5′-triphosphate diphosphohydrolases (eNTPDases, also known

*Author for correspondence; E-mail: george.dubyak@case.edu
Advance online publication: 21 June 2004

as the CD39-family of ecto-apyrases); (2) the ecto-nucleotide pyrophosphatases/phosphodiesterases (eNPPs); (3) the glycosylphosphatidylinositol (GPI)-anchored ecto-5′-nucleotidase (also known as CD73); and (4) the GPI-anchored alkaline phosphatases (APs). The eNTPDase, eNPP, and AP families include multiple subtypes encoded by separate genes. Three members of the eNTPDase/CD39 family (eNTPDase1–3) have been verified as cell surface enzymes that degrade extracellular ATP to ADP, as well as ADP to AMP, releasing inorganic phosphate (P_i). Likewise, three distinct eNPP subtypes (eNPP1–3) hydrolyze ATP directly to AMP and pyrophosphate (PPi). Finally, extracellular AMP can then be degraded to adenosine by either the CD73 ecto-5′nucleotidase or one of four ecto-alkaline phosphatase isoforms (Zimmermann, 2000; Lazarowski *et al*., 2003a).

The identification of ATP synthetic pathways, characterized by ecto-NDPK or ecto-adenylate kinase (ecto-AK) activities, has complicated the interpretation of extracellular ATP accumulation and signaling. Ecto-NDPK activity facilitates the *trans*-phosphorylation of extracellular ADP to ATP using ambient nucleotide triphosphates, such as UTP, GTP, or other nucleotides, as the phosphate donor (Buxton *et al*., 2001; Yegutkin *et al*., 2001; 2002). Although the molecular identity of the eNDPKs has not been defined, they may represent externalized forms of the intracellular NDPKs encoded by the nm23 genes (Lacombe *et al*., 2000; Willems *et al*., 2002; Buckley *et al*., 2003). Ecto-AKs can reversibly convert two extracellular ADP equivalents into ATP and AMP (Picher & Boucher, 2003). Together with the ecto-nucleotidases, the ecto-NDPKs and ecto-AKs serve as important components of the nucleotide-entrapment cycle that can prolong the elevation of ATP and other nucleotides in extracellular compartments (Lazarowski *et al*., 2000; 2003b).

Methylene ATP analogs, such as β,γ-methylene ATP ($\beta\gamma$-meATP) and α,β-methylene ATP ($\alpha\beta$-meATP), possess a methylene group substituted for the oxygen in the phosphodiester bridge between the phosphate moieties of ATP. Since this renders such analogs relatively resistant to hydrolytic attack by nucleotide phosphohydrolases, they have been used either as competitive ecto-ATPase inhibitors or as metabolically stable agonists for certain P2 receptor subtypes (Chen & Lin, 1997; Dowd *et al*., 1999; Yegutkin & Burnstock, 2000; Zimmermann, 2000; Joseph *et al*., 2003; Spelta *et al*., 2003). For example, we have used $\beta\gamma$-meATP, in conjunction with a luciferase-based ATP assay, to inhibit extracellular ATP clearance by 1321N1 human astrocytes and thereby facilitate the measurement of constitutive and stimulated ATP release (Joseph *et al*., 2003). However, it remains unclear whether $\beta\gamma$-meATP acts as a general ecto-ATPase inhibitor or whether it targets particular ecto-ATPase subtypes that are highly expressed by 1321N1 cells. Another analog, $\alpha\beta$-meATP, has been widely used as a relatively selective and stable agonist for ionotropic P2X receptors that contain $P2X_1$ or $P2X_3$ subunits (North, 2002; Spelta *et al*., 2003). This analog also inhibits ecto-ATPases in some cell types (Chen & Lin, 1997; Beigi & Dubyak, 2000; Yegutkin & Burnstock, 2000). Since this analog possesses a hydrolyzable $\beta\gamma$ phosphodiester bond, it might also facilitate ATP synthesis *via* eNDPK activity by phosphate transfer to ambient ADP. This potential action could significantly complicate the interpretation of responses to $\alpha\beta$-meATP in intact tissue preparations.

In this study, we compared the effects of these two methylene ATP analogs on extracellular ATP metabolism in three cell models: (1) human 1321N1 astrocytoma cells that express eNTPDase, eNPP, as well as ecto-NDPK activities (Lazarowski *et al*., 2000); (2) rat PC12 pheochromocytoma cells that predominantly express eNTPDase subtypes (Vollmayer *et al*., 2001); and (3) rat C6 glioma cells that express eNPPs as their major ecto-ATPase (Grobben *et al*., 1999; Ohkubo *et al*., 2001). We demonstrate that both methylene ATP analogs exhibit high selectivity for eNPP- *versus* eNTPDase-family ecto-ATPases. We additionally report that $\alpha\beta$-meATP can significantly increase extracellular ATP in all three cell types by acting as a phosphate donor for eNDPK-catalyzed *trans*-phosphorylation of ambient extracellular ADP.

Methods

Reagents

Firefly luciferase assay mix (FL-AAM), ATP standards (FL-AAS), potato apyrase (grade I), purified NDPK (from baker's yeast), digitonin, and methylene-substituted nucleotide analogs ($\alpha\beta$-meATP, $\beta\gamma$-meATP) were purchased from Sigma-Aldrich, St. Louis, MO, U.S.A. Wild-type 1321N1 human astrocytoma and C6 rat glioma cells were obtained from Drs Ken Harden and Jose Boyer (University of North Carolina, Chapel Hill). PC12 rat pheochromocytoma cells were provided by Dr Gary Landreth (Case Western Reserve University, Cleveland). Total RNA was isolated using TRIzol^R Reagent obtained from Invitrogen Life Technologies, Inc., Carlsbad, CA, U.S.A. Oligo $(dT)_{15}$ Primer (Promega, Madison, WI, U.S.A.) was used for first-strand cDNA synthesis. Reverse transcription reactions and polymerase chain reactions (PCR), respectively, used AMV reverse transcriptase and *Taq* polymerase from Roche, Inc. PCR primers were obtained from Operon-Qiagen, Valencia, CA, U.S.A.

Cell culture

1321N1, C6, and PC12 cell cultures were maintained in Dulbecco's minimal essential medium (DMEM) containing 10% iron-supplemented bovine calf serum (Hyclone), penicillin (100 U ml^{-1}), and streptomycin (100 μg ml^{-1}) (Joseph *et al*., 2003). Unless otherwise stated, the cells were seeded at $\sim 3 \times 10^5$ on 35 mm plastic dishes (Falcon) and grown to confluence for 2 to 3 days (C6 cells) or 5 to 7 days (1321N1 and PC12 cells). At confluence, the dishes contained $\sim 1 \times 10^6$ 1321N1 cells, $\sim 3 \times 10^6$ C6 cells, or $\sim 2 \times 10^6$ PC12 cells.

Assay of extracellular ATP levels by soluble luciferase

All extracellular ATP measurements were performed at room temperature (22–24°C) as described previously (Joseph *et al*., 2003). Briefly, 35 mm dishes containing adherent cell monolayers were washed twice with 2 ml of basal saline solution (BSS) containing (in mM): 130 NaCl, 5 KCl, 1.5 $CaCl_2$, 1 $MgCl_2$, 25 NaHEPES (pH 7.5), 5 glucose, and 0.1% BSA. Cell monolayers were incubated in 1 ml BSS for $\sim$45 min before addition of 40 μl reconstituted FL-AAM containing both luciferase and luciferin. Cell-free calibration curves were generated for each experiment using increasing concentrations of ATP standard (FL-AAS) up to 1000 nM. Under these assay conditions, luciferase-catalyzed bioluminescence was stable at

ATP concentrations $\leqslant 1\,\mu$M. All assays concluded with the addition of digitonin ($50\,\mu g\,ml^{-1}$) to permeabilize the plasma membrane and release cytosolic ATP and thereby provide an estimate of relative cell mass.

Ecto-ATPase inhibition studies

Effects of methylene ATP analogs as ecto-ATPase inhibitors were performed using both luciferase-based and high-performance liquid chromatography (HPLC)-based assays of extracellular ATP metabolism. For luciferase-based analyses, decreases in ATP-dependent luminescence were recorded every 2 min for 10–20 min after addition of 100 nM ATP to cell-free or cell-containing 35 mm dishes as described previously (Joseph *et al*., 2003). Ecto-ATPase inhibition studies were performed using cell monolayers pre-incubated with various concentrations of $\beta\gamma$-meATP or $\alpha\beta$-meATP. For 1321N1 experiments, the methylene ATP analogs were added 15 min prior to baseline recordings, otherwise the analogs were added $\sim$10 s before the addition of exogenous ATP.

Reverse-phase HPLC was used to measure extracellular metabolism of etheno-ATP (εATP) and/or etheno-ADP (εADP), which were employed as highly fluorescent adenine nucleotide analogs (Schafer *et al*., 1978; Mihaylova-Todorova *et al*., 2002). Cell monolayers grown in 24-well plates were washed twice with 1 ml BSS per well before equilibration at RT for $\sim$30 min in 0.5 ml BSS per well. Cells were then preincubated with or without $\beta\gamma$-meATP or $\alpha\beta$-meATP (at various concentrations), prior to addition of $10\,\mu$M εATP or εADP. At selected times, $300\,\mu$l samples of extracellular medium were removed and heated at 100°C for 3 min. Samples were chromatographically resolved on an Alltech C18 Adsorbosphere column, which was eluted at $1.3\,ml\,min^{-1}$ with a methanol gradient formed by mixing limit buffer A (0.1 M KH_2PO_4, pH 6) and limit buffer B (0.1 M KH_2PO_4, pH 6, 15% methanol). The following protocol was used: 0–4 min (100%A); 4–8 min (ramp to 30%A/70%B); 8–25 min (ramp to 100%B), 25–35 min (ramp to 100%A). Absorbance was measured at 260 nm. Simultaneously, the highly fluorescent εATP and its metabolites εADP, εAMP, and ε-adenosine were detected with a Linear LC305 fluorescence detector using 270 nm excitation and 410 nm emission wavelengths.

RT–PCR analysis of ecto-nucleotidase expression

Reverse transcriptase–PCR (RT-PCR) methods were used to compare the expression of ecto-nucleotidase subtype genes in PC12 rat pheochromocytoma *versus* C6 rat glioma cells. Total RNA was extracted from the cell lines using TRIzol™; $10\,\mu$g RNA was primed with random hexamers and incubated with AMV reverse transcriptase and $10\,\mu$M dNTPs at 37°C for 60 min. RT reactions were analyzed for the following cDNA transcripts: (1) ecto-nucleotide triphosphate dihydrolase (eNTPDase/CD39) subtypes eNTPDase1/CD39, eNTPDase2/CD39L2, and eNTPDase3/CD39L3; (2) ecto-nucleotide pyrophosphodiesterase/pyrophosphatase (eNPP) subtypes eNPP1/PC1, eNPP2/autotaxin, and eNPP3/B10/gp130^{RB13-6}; (3) the GPI-anchored CD73 ecto-5′ nucleotidase; and (4) tissue nonspecific ecto-alkaline phosphatase (NS-AP). Table 1 shows the nucleotide sequences for the PCR primer pairs used, as well as the predicted amplicon sizes. These primer pairs were based on published cDNA sequences previously used for RT–PCR analyses of ecto-nucleotidase expression in PC12 or C6 cells (Grobben *et al*., 1999; Ohkubo *et al*., 2001; Vollmayer *et al*., 2001). Glyceraldehyde phosphate dehydrogenase (GAPDH) cDNA amplification was used as a positive control. PCR was performed using 1 : 100 dilutions of the RT reactions in $20\,\mu$l reaction volume containing 10 mM Tris-HCl (pH 8.3), 50 mM KCl, 1.0–1.5 mM $MgCl_2$, $250\,\mu$M premixed deoxynucleotide triphosphates, $0.25\,\mu$M primer mix, and $125\,U\,ml^{-1}$ *Taq* DNA polymerase. The PCR conditions were: 94°C for 2 min, followed by 35 cycles of 94°C for 40 s, 58°C for 40 s, and 74°C for 3 min, with a final extension step of 73°C for 5 min. The resulting PCR amplicons were separated by 1.5% agarose gel electrophoresis and visualized by ethidium bromide staining.

Soluble NDPK substrate assay

Methylene ATP analogs were tested for their ability to act as substrates for soluble NDPK using the luciferase-based assay

Table 1 PCR primer pair sequences for rat ecto-nucleotidases and predicted amplicon sizes

Rat gene	*Strand*	*Primer sequence* (5′–3′)	*Amplicon size (bp)*
ENTPDase1	Sense	GATCATCACTGGGCAGGAGGAAGG	543
	Antisense	AAGACACCGTTGAAGGCACACTGG	
ENTPDase2	Sense	GCTGGGTGGGCCGGTGGATACG	331
	Antisense	ATTGAAGGCCCGGGGACGCTGAC	
ENTPDase3	Sense	CGGGATCCTTGCTGTGCGTGGCATTTCTT	267
	Antisense	TCTAGAGGTGCTCTGGCAGGAATCAGT	
ENPP1	Sense	AGTGCTGTCGCTGGTTTTGT	410
	Antisense	AAGAGAGTAGGGGGTGATTC	
ENPP2	Sense	CGCTCGAGGCTTTCCAAGAATCCCTC	622
	Antisense	CTCTAGACTACACTGCCCAGGCCCA	
ENPP3	Sense	AGCCGCCGGTTATCTTGTTCTC	199
	Antisense	TGATGCCGTGCGACTCTGGATAC	
CD73	Sense	CCCGGGGGCCACTAGCACCTCA	403
	Antisense	GCCTGGACCACGGGAACCTT	
NS-AP	Sense	AAGGGCCAGCTACACCACAACACG	266
	Antisense	GCCCACGGACTTCCCAGCATC	
GAPDH	Sense	TCCACCACCCTGTTGCTGTAGC	401
	Antisense	TGGAAAGCTGTGGCGTGATG	

PCR primer pairs used to assess ecto-nucleotidase subtype expression in rat PC12 pheochromocytoma and rat C6 glioma cells are shown. The primer pairs were based on previously reported sequences (Ohkubo *et al*., 2001; Vollmayer *et al*., 2001).

described above. Cell-free 35-mm dishes contained BSS supplemented with luciferin–luciferase treated with or without methylene analogs (300 μM). For some experiments, the analogs were first pretreated with potato apyrase before being added to the dishes. *De novo* ATP synthesis was then catalyzed using 5 U ml^{-1} of soluble NDPK from baker's yeast. The NDPK-containing solutions with or without methylene ATP analog were then supplemented with ADP substrate added serially to initial concentrations of 3 and 30 μM. At the end of each experiment, exogenous apyrase (5 U ml^{-1}) was used to hydrolyze synthesized ATP. Control studies performed in the absence of added NDPK confirmed that the observed ATP synthesis was NDPK-dependent.

Apyrase treatment of methylene ATP analogs

To test the contribution of contaminating nucleotide triphosphates or diphosphates to the observed actions of the methylene analogs, 500 μl aliquots of 30 mM stocks of each analog were treated with grade I potato apyrase (10 U ml^{-1} in Ca^{2+}/Mg^{2+}-free BSS) for 2.5 h at room temperature. The samples were then boiled for $\sim$5 min to denature the apyrase and centrifuged to remove precipitates or protein aggregates. The apyrase-treated methylene analogs were frozen until used in subsequent ATP luminometric assays. Reverse-phase HPLC, as described above, was used to assess the purity and metabolic lability of the methylene analogs before and after treatment with potato apyrase.

Assay of constitutive extracellular ATP accumulation and cell-associated NDPK activity

The on-line luciferase assay was used to assess extracellular ATP accumulation in 1321N1, PC12, or C6 cell monolayers for up to 20 min in the absence or presence of 300 μM $\beta\gamma$-meATP or $\alpha\beta$-meATP with or without exogenously added ADP (100 nM).

Data evaluation

Most experimental procedures were performed on the same day using duplicate or triplicate dishes of cell monolayers. Experiments were repeated 2–6 times. As previously described, raw luminescence measurements were integrated (for 5 s) to yield relative light unit (RLU) measurements that were downloaded into Microsoft Excel, and converted to ATP concentrations (Joseph *et al*., 2003). Means and standard errors were computed and displayed using the Prism 3.0™ software (GraphPad) and figures were composed using Prism 3.0 (GraphPad) and Illustrator 7.0™ (Adobe) applications software. HPLC experiments were recorded and saved using the Pyramid and DataAlly software packages.

Results

Methylene ATP analogs as inhibitors of 1321N1 ecto-ATPase activity

We previously reported that 300 μM $\beta\gamma$-meATP significantly inhibited the clearance of exogenously added ATP (100 nM) by 1321N1 cell monolayers assayed by an online, luciferase method (Joseph *et al*., 2003). Figures 1a and c illustrate the concentration dependence of this $\beta\gamma$-meATP effect, while Figure 1b demonstrates that 300 μM $\alpha\beta$-meATP also inhibits 1321N1 ecto-ATPase activity by $>$80%. The concentration–response analyses showed that 80% of the ecto-ATPase inhibition by $\beta\gamma$-meATP was produced over a two log-unit range centered at an IC_{50} of $\sim$10 μM. In contrast, 80% of the $\alpha\beta$-meATP inhibitory action was produced over a four log-unit range with a similar IC_{50} (Figure 1c). Neither analog was contaminated with significant ATP nor did either analog have a direct effect on luciferase activity (Figure 1d).

Selective effects of methylene ATP analog on eNPP versus eNTPDase activities

1321N1 cells express eNTPDase, eNPP, and eNDPK activities (Lazarowski *et al*., 2000). Thus, the distinctive concentration–response relationships describing the inhibition of ATP clearance by $\beta\gamma$-meATP *versus* $\alpha\beta$-meATP (Figure 1c) suggested that the two analogs might differentially affect these multiple ecto-enzymes that coordinately regulate extracellular ATP levels. To test this, we compared the actions of $\beta\gamma$-meATP *versus* $\alpha\beta$-meATP on the clearance of extracellular ATP by rat PC12 pheochromocytoma cells *versus* rat C6 glioma cells. Previous studies have demonstrated that PC12 cells mainly express eNTPDase/CD39 family-ectoATPases (Vollmayer *et al*., 2001), while C6 cells primarily express eNPPs as their major ecto-ATPase activity (Grobben *et al*., 1999; Ohkubo *et al*., 2001). We verified that our PC12 line expressed abundant mRNA transcripts for eNTPDases 1, 2, and 3, a low level of tissue nonspecific ecto-alkaline phosphatase (NS-AP) mRNA, but no significant amounts of mRNA encoding eNPP1, eNPP3, or the CD73 ecto-5′nucleotidase (Figure 2). In contrast, our C6 glioma line was characterized by robust expression of mRNAs for eNPP1, eNPP3, and CD73, but no detectable transcripts for eNTPDases 1–3. The observed 210 bp amplicons for the eNPP2 PCR reactions from both cell types were smaller than the predicted 622 bp product indicating nonspecific amplification by these primer pairs. Regardless of its relative expression level, eNPP2 is unlikely to contribute a major ecto-ATPase activity given recent reports that eNPP2 (autotaxin) functions primarily as an ecto-phospholipase D for generating extracellular lysophospholipids, rather than as an ecto-nucleotidase (Umezu-Goto *et al*., 2002; Gijsbers *et al*., 2003).

At 300 μM, $\beta\gamma$-meATP and $\alpha\beta$-meATP reduced the PC12-mediated clearance of added ATP (100 nM) by only $\sim$10 and $\sim$50%, respectively (Figure 3a). In contrast, both analogs significantly ($>$95%) inhibited ATP clearance by C6 glioma (Figure 3b), similar to their effects on the 1321N1 cells. The data indicate that these methylene analogs – $\beta\gamma$-meATP, in particular – preferentially target eNPP family ecto-ATPases (eNPP1 and/or 3) over the CD39 family eNTPDases. This selectivity is species-independent because both human (1321N1) and rat (C6) ecto-ATPases were similarly inhibited by the analogs (compare Figures 1 and 3).

The experiments illustrated in Figures 1 and 3 utilized the luciferase-based assay that facilitates continuous readout of extracellular [ATP] in the nanomolar through submicromolar range. These ATP concentrations are lower than the 10–100 μM K_m values that characterize ATP utilization by the various ecto-nucleotidase subtypes (Zimmermann, 2000).

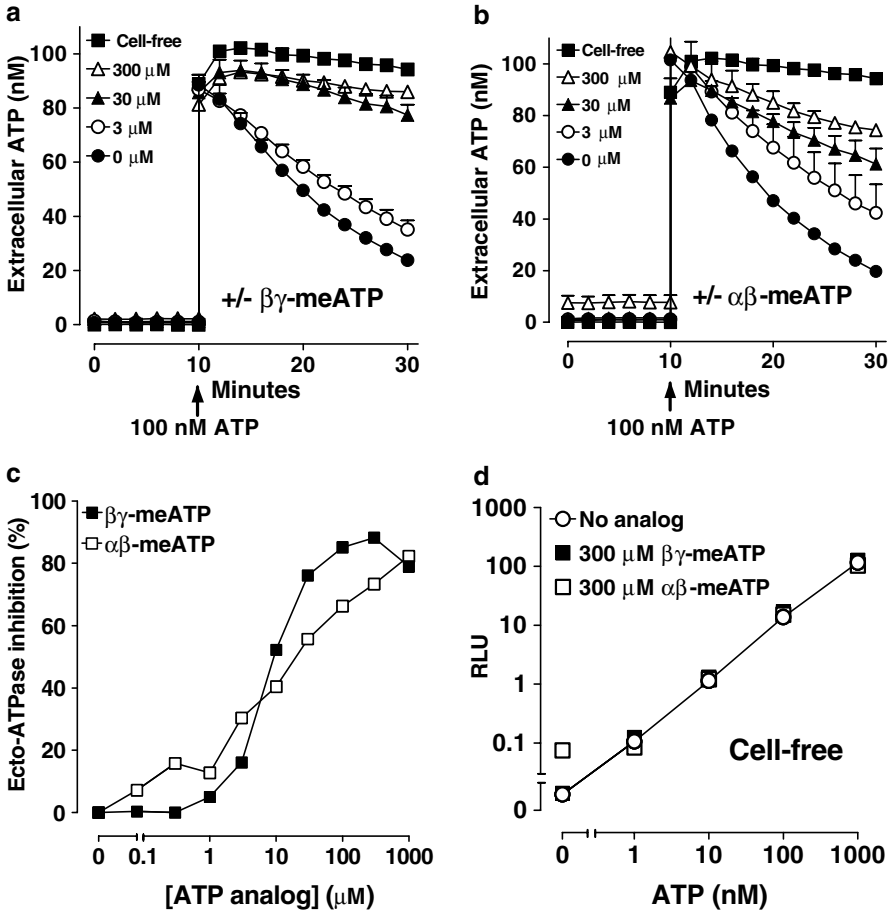

Figure 1 Effects of $\beta\gamma$-meATP or $\alpha\beta$-meATP on ecto-ATPase activity of human 1321N1 astrocytes. Extracellular ATP concentration was measured in monolayer cultures (35 mm dishes) of 1321N1 astrocytes bathed in 1 ml of assay medium using the luciferase-based protocol described in Methods. (a and b) Cells were incubated with the indicated concentrations of $\beta\gamma$-meATP (Panel a) or $\alpha\beta$-meATP (Panel b) for 10 min prior to addition of luciferin–luciferase. ATP measurements were made for 10 min before addition of 100 nM exogenous ATP. ATP clearance was assayed over the next 20 min. Cell-free culture dishes were identically assayed to demonstrate the minimal rate of ATP clearance by the luciferase ATP sensor under these experimental conditions. Data points in panels a and b represent the mean $\pm$ s.e.m. of three and two experiments, respectively. The average content of endogenous diffusible ATP, measured after digitonin-mediated permeabilization of each monolayer, was 4.4 ± 0.21 nmol for the panel a experiments and 5.8 ± 0.42 nmol for the panel b experiments. (c) Data from experiments similar to those in panels a and b were used to calculate the percent inhibition of ecto-ATPase activity (based on the difference between the observed rates of ATP clearance by untreated *versus* analog-treated cells); this was plotted as a function of $\beta\gamma$-meATP or $\alpha\beta$-meATP concentration. (d) Calibration curves for luciferase activity as a function of increasing ATP concentration in the absence or presence of 300 μM $\beta\gamma$-meATP or $\alpha\beta$-meATP were plotted using identical experimental conditions as in panels a–c but with cell-free culture dishes. A representative calibration curve is shown.

However, luciferase is not well-suited for quantitation of ATP concentrations in this latter K_m range due to product inhibition that leads to nonlinear flash-kinetics (Ford *et al*., 1996). To further characterize the selectivity of the methylene analogs for eNPPs, we used an HPLC-based method to measure the inhibitory action of $\beta\gamma$-meATP using an ATP substrate concentration (10 μM) that approximates the reported K_m values for eNPPs (Bollen *et al*., 2000; Lazarowski *et al*., 2000). To facilitate effective chromatographic analysis of the 10 μM ATP substrate in presence of the 300 μM $\beta\gamma$-meATP inhibitor, we employed the fluorescent analog etheno-ATP (εATP) as substrate (Schafer *et al*., 1978; Mihaylova-Todorova *et al*., 2002). This allowed simultaneous use of fluorescence detection to measure εATP metabolism and absorbance detection to assay $\beta\gamma$-meATP metabolism (Figure 4). C6 glioma cells efficiently metabolized εATP into ε-adenosine (εAdo) with little accumulation of the εADP or εAMP intermediates during a 60-min incubation (Figure 4c); this pattern was indicative of the concerted actions of the eNPP and CD73 (AMPase) activities. This metabolism of εATP to εAdo by the C6 cells was markedly attenuated in the presence of 300 μM $\beta\gamma$-meATP (Figure 4e). Consistent with previous findings (Ohkubo *et al*., 2001), C6 cells significantly metabolized $\beta\gamma$-meATP to AMP and Ado such that $\sim$8 % of the analog was degraded after 60 min (Figure 4f). Thus, the ability of $\beta\gamma$-meATP to repress the ecto-ATPase activity of eNPP1/3 appears correlated with its ability to act as a substrate for these enzymes. However, detailed kinetic analysis would be required to determine whether $\beta\gamma$-meATP acts as a *bona fide* competitive inhibitor of eNPPs. In contrast, PC12 cells hydrolyzed εATP primarily to εADP

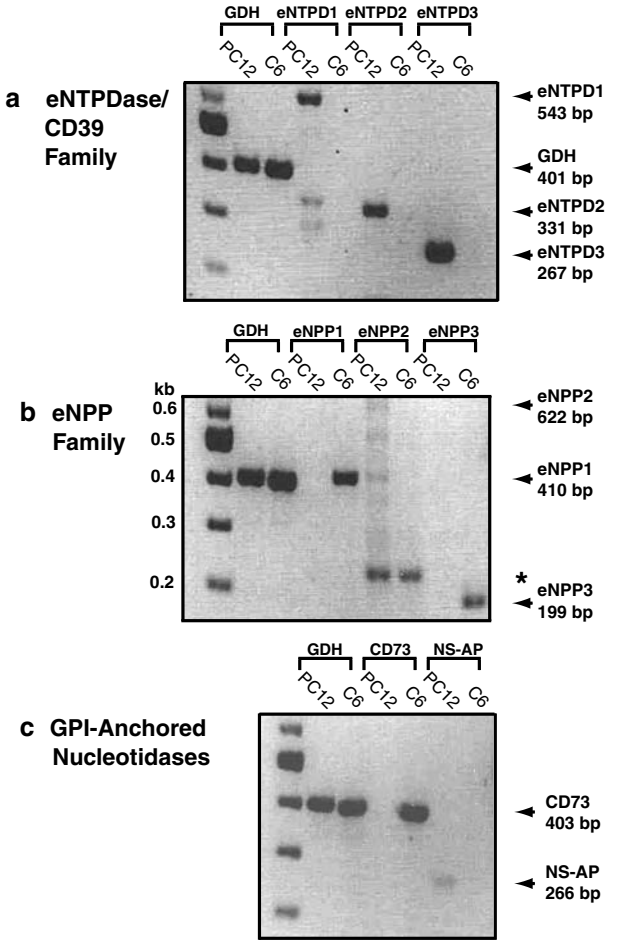

Figure 2 Differential expression of genes encoding known ecto-ATPases and ecto-nucleotidases in PC12 pheochromocytoma *versus* C6 glioma cells. RNA from PC12 or C6 cells was analyzed by RT–PCR for transcripts corresponding to the three known cell surface eNTPDase/CD39 subtypes (panel a); the three known eNPP subtypes (panel b); or CD73 and nonspecific alkaline phosphatase (NS-AP), the two GPI-anchored ecto-nucleotidases (panel c). Each representative electrophorogram compares side-by-side the RT–PCR reaction products for PC12- *versus* C6-derived RNA together with DNA size markers and the GAPDH RT – PCR products as positive controls. (*) indicates the major amplicon observed with the eNPP2 primer pairs that was much smaller than the predicted 622 bp amplicon.

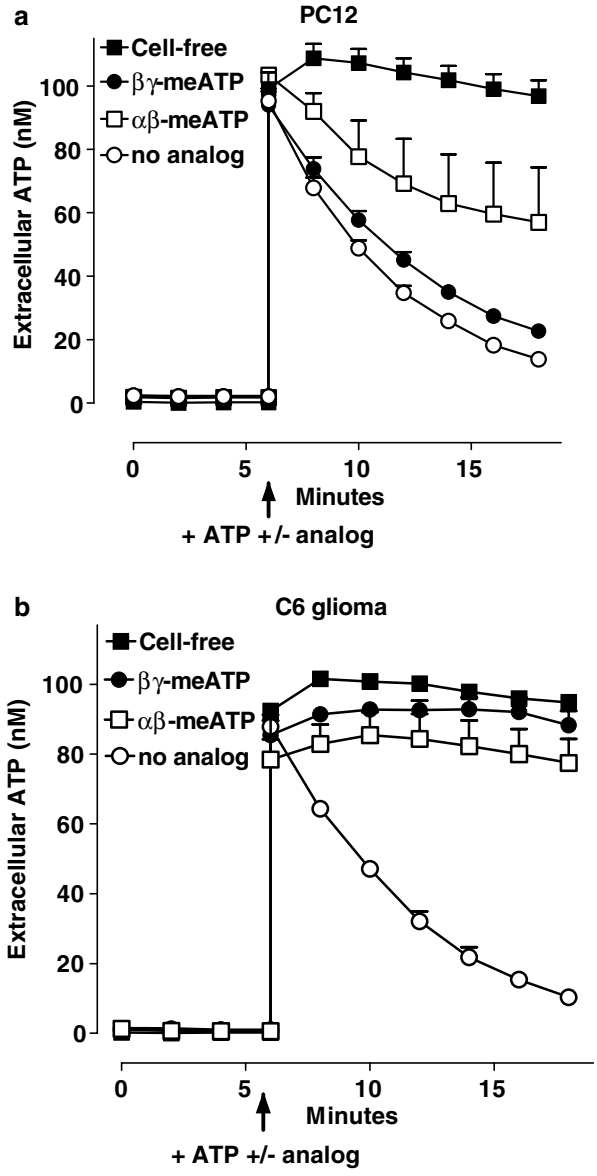

Figure 3 Differential inhibitory effects of $\beta\gamma$-meATP and $\alpha\beta$-meATP on ecto-ATPase activity of rat PC12 *versus* rat C6 cells. Extracellular ATP concentration was measured in monolayer cultures (35 mm dishes) of PC12 cells (panel a) or C6 cells (panel b) bathed in 1 ml of assay medium using the luciferase-based protocol described in Methods. (a and b) Cells were incubated with 300 μM $\beta\gamma$-meATP or 300 μM $\alpha\beta$-meATP prior to addition of 100 nM ATP; ATP clearance was assayed over the next 12 min. Cell-free culture dishes were identically assayed to demonstrate the minimal rate of ATP clearance by the luciferase ATP sensor under these experimental conditions. Data points in panel a represent the mean $\pm$s.e.m. of 2–6 experiments while the data points in panel b represent mean $\pm$s.e.m. of four experiments. The average content of endogenous ATP, measured after digitonin-induced permeabilization of each monolayer was 0.46 ± 0.05 nmol for the PC12 monolayers and 2.25 ± 0.10 nmol for the C6 monolayers.

and εAMP (Figure 4g). Negligible ε-adenosine was produced by these cells, consistent with the lack of CD73 and low NS-AP mRNA expression (see Figure 2c). $\beta\gamma$-meATP had negligible effects on this metabolism of εATP by the PC12 eNTPDases (Figure 4i) and $\beta\gamma$-meATP itself was not degraded (Figure 4j).

These data indicate that $\beta\gamma$-meATP will act as an efficacious ecto-ATPase inhibitor when eNPPs, rather than eNTPDases, are the principal ecto-ATPase in a given cell or tissue system. This is readily apparent in a cell type, such as C6, that expresses eNPPs to the exclusion of eNTPDase subtypes. In cells such as 1321N1, that express both eNPPs and eNTPDases, the observed ability of $\beta\gamma$-meATP to completely repress the clearance of submicromolar ATP (Figure 1) suggests that eNPPs provide the major ecto-ATPase activity for the scavenging of basally or constitutively released ATP (Lazarowski *et al*., 2000).

Methylene ATP analogs as NDPK substrates

The ability of $\alpha\beta$-meATP to partially attenuate ATP clearance by PC12 cells (Figure 3a) suggested that this analog might also act as an eNTPDase inhibitor. Alternatively, this observation might indicate that the hydrolysis of ATP was opposed by an

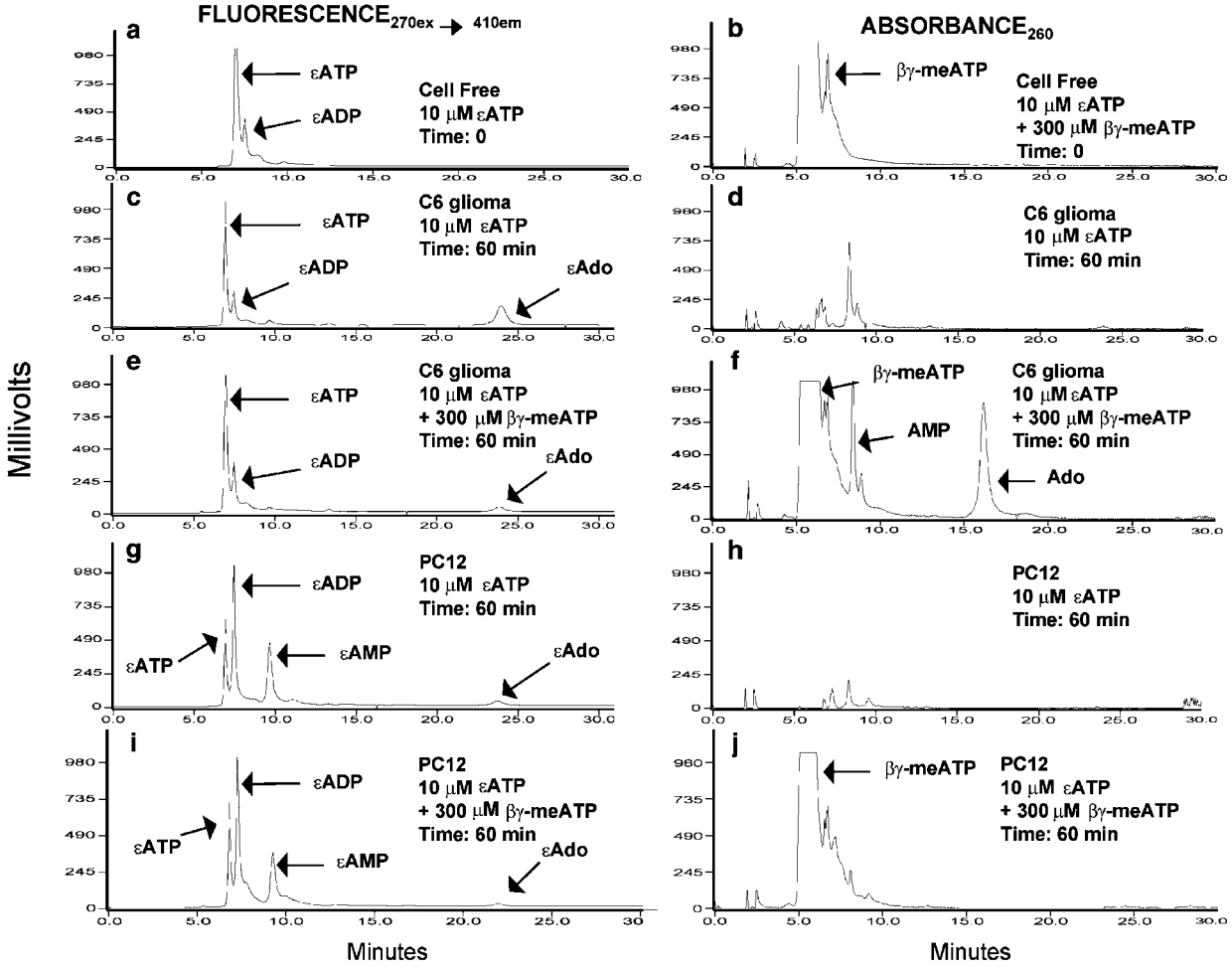

Figure 4 $\beta\gamma$-meATP acts as a competitive substrate to repress extracellular metabolism of εATP by C6 cells but not PC12 cells. Monolayers of C6 cells (c, d, e, f) or PC12 cells (g, h, i, j) plated in 24-well culture dishes, were incubated with 10 μM εATP, as a highly fluorescent ATP analog, for 60 min in the absence (c, d, g, h) or presence (e, f, i, j) of 300 μM $\beta\gamma$-meATP. Aliquots of the extracellular media were then processed and analyzed by reversed-phase HPLC as described in Methods. Chromatograms in the left panels illustrate the fluorimetric (270 nm excitation; 410 nm emission) detection of εATP, εADP, εAMP, and ε-adenosine (εAdo) in media samples from C6 cells (c, e) *versus* PC12 cells (g, i) while chromatograms in the right panels illustrate absorbance (260 nm) detection of $\beta\gamma$-meATP, AMP, and adenosine in the same media samples from C6 cells (d, f) or PC12 cells (h, j). Amounts of 10 μM εATP and 300 μM $\beta\gamma$-meATP added to test medium in the absence of cell monolayers (a, b) were used as zero-time samples.

increased ATP synthesis due to an eNDPK-catalyzed transphosphorylation of ambient ADP in the presence of $\alpha\beta$-meATP. Ecto-NDPK activity has been described in a variety of cell types, including 1321N1 astrocytes, endothelial cells, C6 glioma, and osteoblasts (Lazarowski *et al*., 2000; Buxton *et al*., 2001; Yegutkin *et al*., 2001; Buckley *et al*., 2003). Figure 5a schematically indicates how ATPases facilitate the hydrolysis of ATP to ADP and inorganic phosphate (P_i) while NDPKs catalyze *de novo* ATP synthesis by transferring the γ-phosphate moiety from nucleoside triphosphates to ADP. We used the luciferase-based ATP assay for *in vitro* analysis of purified yeast NDPK activity (5 U ml^{-1} soluble enzyme) in the presence of 300 μM $\alpha\beta$-meATP or $\beta\gamma$-meATP as phospho-donors, and ADP (3 or 30 μM) as the phospho-acceptor (Figure 5b). Negligible ATP synthesis was observed with $\beta\gamma$-meATP consistent with the nontransferable nature of its methyl-bound γ-phosphate. In contrast, $\alpha\beta$-meATP supported the significant phosphorylation of ADP and this ATP synthesis was strictly dependent on the presence of NDPK. Similar NDPK experiments were performed using methylene ATP analogs pretreated with potato apyrase, a nucleoside triphosphate-scavenging enzyme. Apyrase treatment abrogated the ATP synthesis driven by $\alpha\beta$-meATP enzyme (Figure 5c) and HPLC analysis confirmed that this was due to the quantitative conversion of $\alpha\beta$-meATP to $\alpha\beta$-meADP (data not shown).

The latter observations suggested that $\alpha\beta$-meATP can act as a substrate for the ecto-NDPKs expressed by many cell types. This was tested using intact 1321N1 cell monolayers incubated for 60 min with ε-ADP, as a fluorescent ADP phospho-acceptor, in the presence or absence of $\alpha\beta$-meATP or $\beta\gamma$-meATP (Figure 6). In the absence of the methylene analogs, ε-ADP was largely metabolized to ε-adenosine, consistent with the serial actions of an eNTPDase/ecto-apyrase and CD73 ecto-5′nucleotidase (Figure 1c). This pattern of ε-ADP metabolism was not altered in the presence of 300 μM $\beta\gamma$-meATP, consistent with the insensitivity of eNTPDase/ecto-apyrases to this analog (Figure 6g). Nonetheless, some $\beta\gamma$-meATP was metabolized to adenosine due to the serial actions

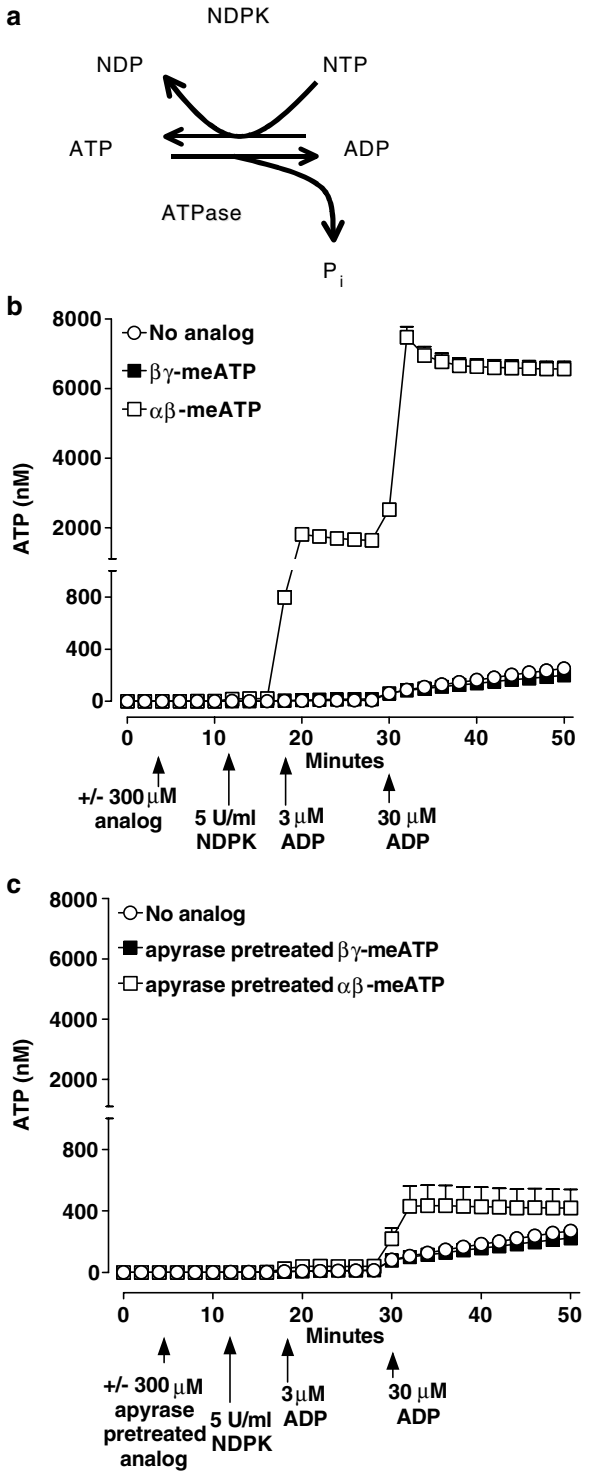

Figure 5 $\alpha\beta$-meATP, but not $\beta\gamma$-meATP, acts as a phospho-donor substrate for purified yeast NDPK. (a) Scheme showing role of NDPK as an ATP synthesizing enzyme that opposes the actions of ATPases which degrade ATP. (b) The (cell-free) luciferase assay system was used to measure ATP synthesis catalyzed by yeast NDPK in the presence of 300 μM $\beta\gamma$-meATP or $\alpha\beta$-meATP as phospho-donors in response to the addition of 3 or 30 μM exogenous ADP as the phospho-acceptor. Baker's yeast NDPK was dissolved in the same basal salt solution used in the analyses of extracellular ATP metabolism by intact cells. Data points represent the mean $\pm$s.e.m. of six experiments. (c) NDPK reactions identical to those illustrated in panel b were performed using $\beta\gamma$-meATP or $\alpha\beta$-meATP that was pretreated with potato apyrase. Data points represent the average values from two experiments.

of eNPP and CD73 activities (Figure 6h). Importantly, we observed that $\alpha\beta$-meATP supported the synthesis of εATP from exogenous εADP (Figure 6e). A similar response was observed when C6 glioma or PC12 cells were coincubated with ε-ADP and $\alpha\beta$-meATP (data not shown).

Effects of methylene ATP analogs on extracellular ATP accumulation by 1321N1, PC12, and C6 glioma cells at steady state

Most cultured cell types maintain a nanomolar concentration of extracellular ATP in their bathing medium due to a steady-state balance that reflects a constitutive ATP release opposed by a basal rate of ATP hydrolysis (Lazarowski *et al*., 2000). Figure 7 shows that 1321N1, C6, and PC12 monolayers steadily maintain extracellular ATP at 0.5–1 nM when similarly assayed using the on-line luciferase method. Given a constitutive release of ATP, any inhibition of basal ecto-ATPase activity should cause a rise in extracellular ATP to a new steady-state value. Consistent with its selective inhibitory action on eNPP activity, $\beta\gamma$-meATP induced a 3–4-fold elevation of extracellular ATP in 1321N1 and C6 monolayers (Figures 7a and c), but not in PC12 cells (Figure 7b). Surprisingly, under the same assay conditions, $\alpha\beta$-meATP caused 10–20-fold increases in extracellular ATP in PC12 monolayers and 1321N1 cells, but only a three-fold elevation in the C6 cultures.

The greater efficacy of $\alpha\beta$-meATP (relative to $\beta\gamma$-meATP) in supporting steady-state ATP accumulation by 1321N1 and PC12 monolayers indicated a possible contribution of eNDPK-mediated ATP synthesis consistent with the HPLC data illustrated in Figure 6. The ability of $\alpha\beta$-meATP to increase ATP in the absence of exogenously added ADP further implied that 1321N1 and PC12 cultures accumulate significant amounts of extracellular ADP derived from endogenous stores. The absence of a robust ATP accumulation response to $\alpha\beta$-meATP by the C6 cells suggested that these cells maintain lower levels of extracellular ADP at steady state. This would be consistent with the expression of eNPPs – which directly hydrolyze ATP to AMP – as the predominant ATP scavenging ectoenzymes in C6 cells. To test this, we compared $\alpha\beta$-meATP-induced ATP accumulation among the three cell types in the presence or absence of exogenously added 100 nM ADP (Figure 8a–c). When supplemented with exogenous ADP, all three cell types exhibited a >30-fold rise in extracellular ATP accumulation in response to addition of 300 μM $\alpha\beta$-meATP. Varying the added $\alpha\beta$-meATP from 1 up to 300 μM in 1321N1 cultures produced a concentration-dependent increase in accumulated ATP with 10 μM $\alpha\beta$-meATP driving the steady-state synthesis of 10 nM ATP in the presence of 100 nM ADP (Figure 8d). This induced ATP synthesis was not observed upon coexposure to $\beta\gamma$-meATP and ADP (not shown). Thus, $\alpha\beta$-meATP, which is widely used for selective activation of $P2X_1$ and $P2X_3$ receptors, can secondarily induce accumulation of ATP, an agonist for a much broader range of P2X and P2Y subtypes. It is also possible that $\alpha\beta$-meATP might additionally stimulate release of endogenous ATP stores secondary to activation of various P2X receptors in certain cell types. However, this is an unlikely complication in the case of 1321N1 astrocytes that lack expression of any known P2X or P2Y receptor subtypes.

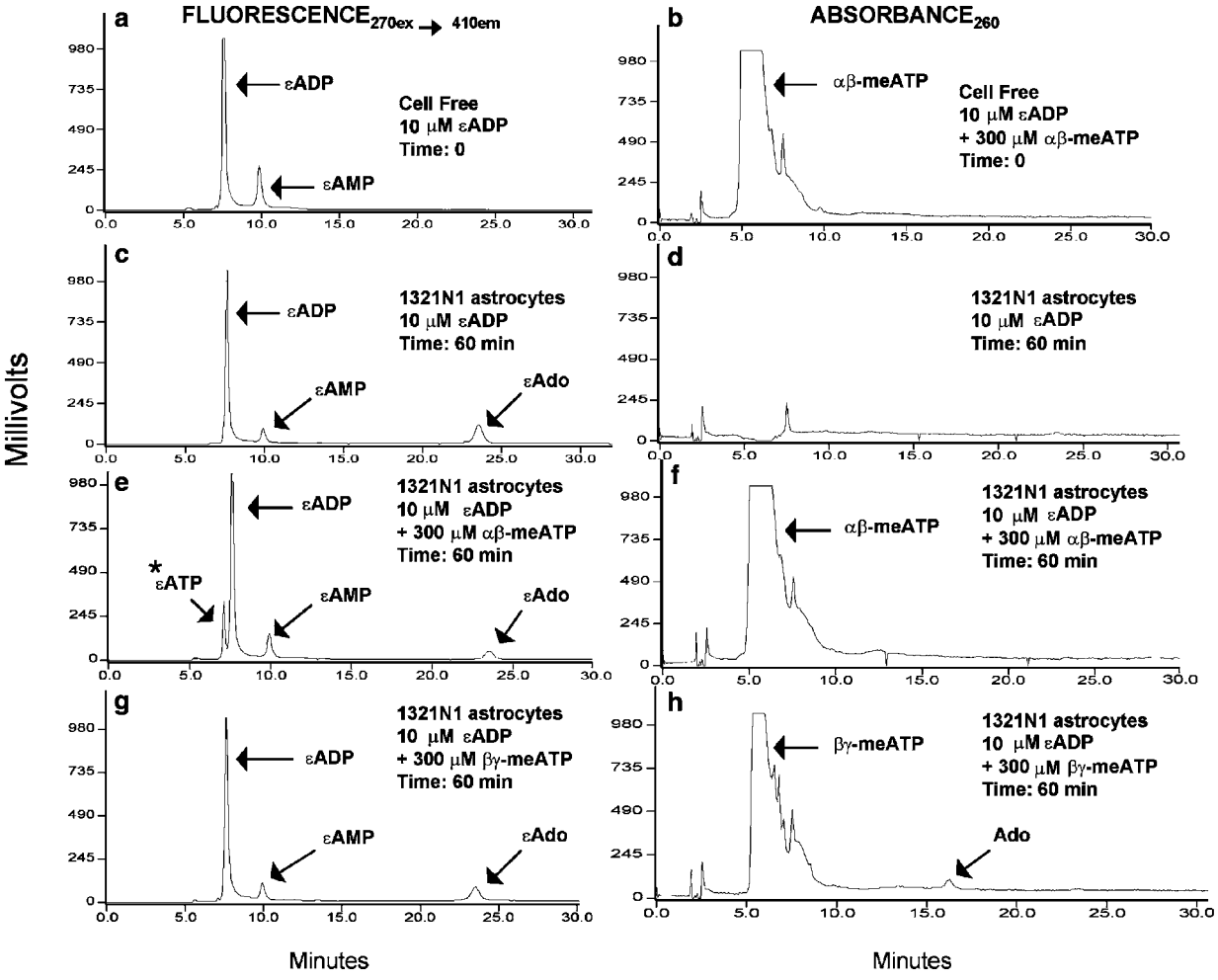

Figure 6 $\alpha\beta$-meATP, but not $\beta\gamma$-meATP, acts as a phospho-donor substrate for the ecto-NDPK activity expressed in 1321N1 astrocytes. Monolayers of 1321N1 cells plated in 24-well culture dishes, were incubated with 10 μM εADP, as a highly fluorescent ADP analog, for 60 min alone (c, d) or in the presence of 300 μM $\alpha\beta$-meATP (e, f) or 300 μM $\beta\gamma$-meATP (g, h). Aliquots of the extracellular media were then processed and analyzed by reversed-phase HPLC as described in Methods. Chromatograms in the left panels (a, c, e, g) illustrate the fluorimetric (270 nm excitation; 410 nm emission) detection of εATP, εADP, εAMP, and ε-adenosine (εAdo) in media samples while chromatograms in the right panels (b, d, f, h) illustrate absorbance (260 nm) detection of $\alpha\beta$-meATP, $\beta\gamma$-meATP, or adenosine in the same media samples. Amounts of 10 μM εADP and 300 μM $\alpha\beta$-meATP added to test medium in the absence of cell monolayers (a, b) were used as zero-time samples. (*) shows the *de novo* εATP synthesized by the $\alpha\beta$-meATP-driven phosphorylation of εADP.

Discussion

This study describes several new findings regarding the pharmacological effects of methylene ATP analogs on extracellular nucleotide metabolism. Analysis of three different cell types demonstrated that $\beta\gamma$-meATP selectively inhibits ATP hydrolysis catalyzed by ecto-nucleotide pyrophosphatase (eNPP) *versus* ecto-nucleoside 5′-triphosphate diphosphohydrolase (eNTPDase) activities. Other experiments revealed that $\alpha\beta$-meATP can act as both an ecto-ATPase inhibitor and a phosphodonor for the eNDPK-catalyzed phosphorylation of extracellular ADP to ATP. As schematically illustrated in Figure 9, such effects on extracellular ATP metabolism may markedly complicate interpretation of integrated purinergic responses by different tissues exposed to these methylene analogs. Thus, these findings indicate that the unambiguous use of $\alpha\beta$-meATP and $\beta\gamma$-meATP as either ecto-ATPase inhibitors or P2 receptor agonists requires some *a priori* knowledge of the P2 receptor subtypes and nucleotide-directed ecto-enzymes expressed by the various cell types that comprise a tissue.

Our specific experimental observations also raise some general implications regarding the possible localization of various ecto-nucleotidases, P2 receptors, adenosine receptors, and ATP release sites within purinergic signaling complexes on cell surfaces. We have previously described the use of $\beta\gamma$-meATP to repress an ecto-ATPase activity that was functionally colocalized with sites of endogenous ATP release in 1321N1 astrocytes (Joseph *et al.*, 2003). These new experiments indicate that this colocalized ecto-ATPase activity is an eNPP. Moreover, 1321N1 and C6 cells rapidly metabolized $\beta\gamma$-meATP to adenosine by a tightly coupled reaction involving serial catalysis by eNPP ($\beta\gamma$-meATP→AMP) and CD73 (AMP→adenosine) activities. This indicates that the inhibitory effect of $\beta\gamma$-meATP on hydrolysis of endogenously released ATP is correlated with its action as a substrate for

eNPPs. Taken together, our previous and current studies suggest that eNPPs may be compartmentalized within plasma membrane subdomains that additionally contain CD73 and sites of endogenous ATP release. This possibility is consistent with recent observations by Ohkubo and colleagues who demonstrated that exposure of either C6 cells or *Xenopus* oocytes to $\beta\gamma$-meATP triggered rapid activation of adenosine receptors by a serial reaction cascade involving both eNPP1/PC-1 and CD73 (Ohkubo *et al*., 2001; Matsuoka *et al*., 2002). Thus, our observations regarding compartmentalized effects of $\beta\gamma$-meATP on the accumulation and metabolism of extracellular nucleotides add to a growing literature regarding an apparent colocalization of ATP release sites, ecto-nucleotidases, P2 receptors, and adenosine receptors within specialized subdomains of the plasma membrane (Koziak *et al*., 2000; Lasley *et al*., 2000; Kaiser *et al*., 2002; Joseph *et al*., 2003).

Previous studies have shown that $\alpha\beta$-meATP and $\beta\gamma$-meATP can exhibit different properties as ecto-ATPase inhibitors in various preparation or tissue types (Chen & Lin, 1997; Yegutkin & Burnstock, 2000). Significantly, Picher *et al*. (1996) reported that $\alpha\beta$-meATP and $\beta\gamma$-meATP similarly inhibited (K_i values of 18 and 17 μM, respectively) a detergent-solubilized ecto-NTPDase purified from bovine aorta. The ability of these methylene analogs to inhibit effectively a solubilized CD39-type enzyme contrasted with our observation that these compounds were poor inhibitors of the *in situ* CD39 enzyme activity in PC12 cells. This suggests that recognition of these methylene-ATP derivatives by various ecto-nucleotidase subtypes is additionally influenced by the physical state of the ecto-enzymes. It remains to be tested whether these analogs might exhibit selective effects on particular subtypes of intact eNPPs or solubilized eNTPDases, similar to the subtype-selective actions of Evans blue and suramin as inhibitors of NTPDase-1 and NTPDase-2, respectively (Heine *et al*., 1999).

The use of $\alpha\beta$-meATP as a selective agonist for $P2X_1$- or $P2X_3$-containing channels has been extensively documented and reviewed (North, 2002). Spelta *et al*. (2003) have recently compared the effects of a broad range of methylene-phosphate-substituted ATP analogs on the activation of recombinant $P2X_{2/3}$ receptors. These studies revealed that only $\alpha\beta$-meATP was a potent $P2X_{2/3}$ agonist (EC_{50} $\sim$3 μM) with $\beta\gamma$-meATP being a low-potency partial agonist (EC_{50} $\sim$200 μM) (Spelta *et al*., 2003). However, our finding that $\alpha\beta$-meATP can be utilized by eNDPKs for the phosphorylation of ambient nucleoside diphosphates indicates that integrated responses of complex tissues to $\alpha\beta$-meATP (e.g., smooth muscle contraction) may reflect activation of P2 subtypes in

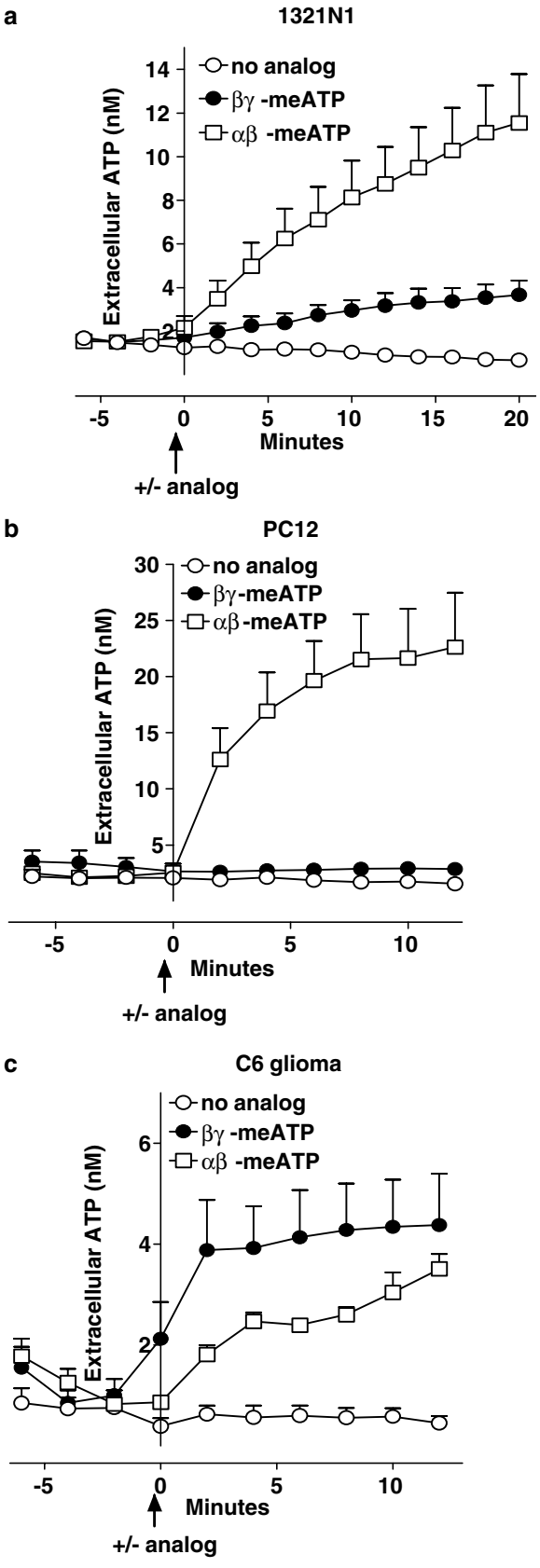

Figure 7 Differential stimulatory effects of $\beta\gamma$-meATP *versus* $\alpha\beta$-meATP on the constitutive accumulation of extracellular ATP in monolayer cultures of 1321N1, PC12, and C6 cells. Extracellular ATP concentration was measured in monolayer cultures (35 mm dishes) of 1321N1 cells (panel a), PC12 cells (panel b), or C6 cells (panel c) bathed in 1 ml of assay medium using the luciferase-based protocol described in Methods. After baseline luciferase activity reached a steady value, cells were left untreated or were exposed to 300 μM $\beta\gamma$-meATP or 300 μM $\alpha\beta$-meATP. Changes in accumulation of extracellular ATP were followed over the next 10–20 min. Data points represent the mean $\pm$s.e.m. of 3–4 experiments. The average content of endogenous ATP, measured after digitonin-mediated permeabilization of each monolayer was 7.3$\pm$0.3 nmol for the 1321N1 monolayers; 0.6$\pm$0.1 nmol for the PC12 monolayers; and 2.6$\pm$0.4 nmol for the C6 monolayers.

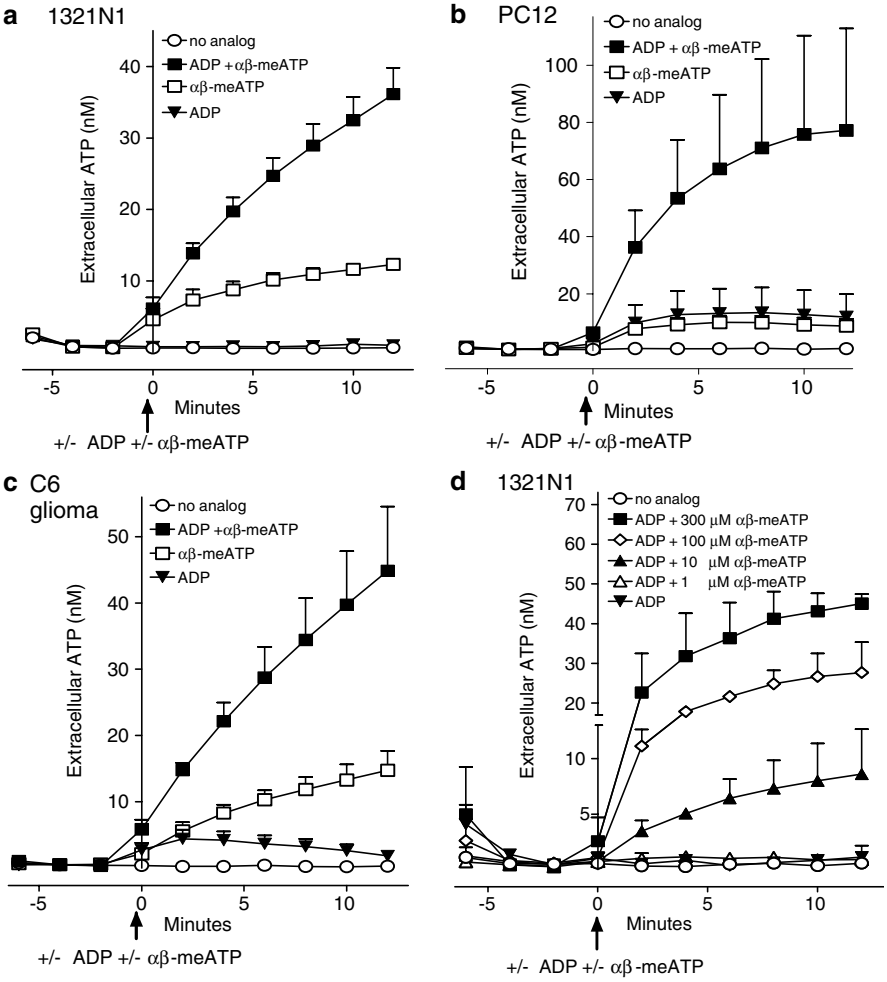

Figure 8 $\alpha\beta$-meATP as a phospho-donor for ecto-NDPK catalyzed phosphorylation of endogenous *versus* exogenous ADP in monolayer cultures of 1321N1, PC12, and C6 cells. Extracellular ATP concentration was measured in monolayer cultures (35 mm dishes) of 1321N1 cells (panel a), PC12 cells (panel b), or C6 cells (panel c) bathed in 1 ml of assay medium using the luciferase-based protocol described in Methods. After baseline luciferase activity reached a steady value, cells were left untreated or were exposed to 300 μM $\alpha\beta$-meATP in the absence or presence of 100 nM exogenously added ADP. Changes in accumulation of extracellular ATP were followed over the next 15 min. In panel d, 1321N1 cells were treated with increasing $\alpha\beta$-meATP concentrations in the presence of 100 nM ADP. Data points represent the mean $\pm$s.e.m. of 2–4 experiments. The average content of endogenous ATP, measured after digitonin-induced permeabilization of each monolayer was 4.5 ± 1.6 nmol for the 1321N1 monolayers; 0.58 ± 0.1 nmol for the PC12 monolayers; and 1.8 ± 0.4 nmol for the C6 monolayers.

addition to $P2X_1$, $P2X_3$, or $P2X_{2/3}$ receptors. For example, the rapid phosphorylation of ambient UDP (Lazarowski *et al*., 1997) following exposure to $\alpha\beta$-meATP could activate the $P2Y_2$ and $P2Y_4$ receptors that are often coexpressed with $P2X_1$ or $P2X_{2/3}$ receptors in excitable or vascular tissues (Ralevic & Burnstock, 1998). When $\alpha\beta$-meATP and $\beta\gamma$-meATP are utilized as P2 receptor agonists, they are generally tested in the 1–100 μM concentration range. Our experiments with 1321N1 astrocytes indicated that the IC_{50} for $\beta\gamma$-meATP as an ecto-NPP inhibitor was in the 10 μM range (Figure 1c), while 10–100 μM $\alpha\beta$-meATP was sufficient to drive the ecto-NDPK-catalyzed accumulation of extracellular ATP (Figure 8d).

ARL67156 (6-*N*,*N*-diethyl-D-$\beta\gamma$-dibromomethylene-ATP, formerly FPL67156) is another methylene ATP derivative that has been widely used as an ecto-ATPase inhibitor, which lacks agonistic activity at P2X or P2Y receptors (Crack *et al*., 1995; Dowd *et al*., 1999; Connolly & Duley, 2000; Sneddon *et al*., 2000; Zimmermann, 2000; Newman, 2003). However, little is known regarding the possible selectivity of this analog on the eNTPDase- *versus* the eNPP-family ecto-ATPases. Using the luciferase-based assay of ecto-ATPase activity, we observed that 300 μM ARL67156 only partially inhibited (by 50–70%) the rate of ATP clearance by intact monolayers of 1321N1 astrocytes, PC12, or C6 glioma cells (data not shown). Previous studies have similarly observed that ARL67156, even at submillimolar levels, is unable to completely repress ecto-ATPase activity in preparations from rat parotid gland (Dowd *et al*., 1999), guinea-pig vas deferens (Mihaylova-Todorova *et al*., 2002), and human blood cells (Crack *et al*., 1995). The similar actions of ARL67156 on ecto-ATPase activities of both C6 and PC12 cells suggest that this reagent acts as a modestly efficacious inhibitor of both eNPP- and eNTPDase-type nucleotidases. If ARL67156, like $\beta\gamma$-meATP, can be appreciably metabolized by eNPP-family enzymes, then the use of this reagent may additionally be complicated by the generation of nucleoside metabolites with uncertain actions on adenosine receptors.

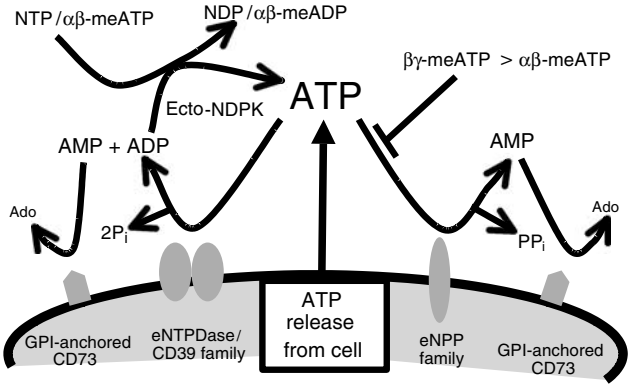

Figure 9 Schematic summary of the effects of $\beta\gamma$-meATP and $\alpha\beta$-meATP on extracellular ATP metabolism. In resting cells, ATP may accumulate in the extracellular compartment *via* ATP release or by ecto-NDPK-mediated *de novo* ATP synthesis. The latter occurs by a *trans*-phosphorylation reaction between ambient ADP and nucleotide triphosphates that contain a hydrolyzable β-γ phosphodiester bond, such as $\alpha\beta$-meATP. Both $\beta\gamma$-meATP and $\alpha\beta$-meATP are more effective inhibitors of ATP degradation mediated by eNPPs than by eNTPDases. CD73 functions to scavenge the resultant AMP to Ado.

These findings emphasize the need for high-efficacy, non-nucleotide inhibitors of the multiple ecto-nucleotidases that shape the magnitude and duration of P2 receptor-based signaling responses during physiological cell-to-cell communication. Previous studies have utilized PPADS (pyridoxalphosphate-6-azophenyl-2′,4′-disulphonate), reactive blue 2, Evans blue, suramin, and naphthol derivatives as non-nucleotide inhibitors of ecto-ATPase activities in diverse cell types (Chen *et al*., 1996; Grobben *et al*., 1999; Heine *et al*., 1999; Gendron *et al*., 2002; Jacobson *et al*., 2002). However, all of these reagents also directly antagonize a broad range of P2Y or P2X receptor subtypes. Thus, the development of non-nucleotide ecto-nucleotidase inhibitors that lack activity at P2 receptors remains a high priority for the study and manipulation of purinergic/pyrimidinergic signaling in complex tissues.

We thank Michelle Kahlenberg and Reza Beigi for discussions and comments and Sylvia Kertesy for technical assistance. This study was supported by NHLBI P01-HL18708 from the National Institutes of Health and Grant-in Aid 9950305N from the American Heart Association (National).

References

BEIGI, R.D. & DUBYAK, G.R. (2000). Endotoxin activation of macrophages does not induce ATP release and autocrine stimulation of P2 nucleotide receptors. *J. Immunol.,* **165,** 7189–7198.

BOLLEN, M., GIJSBERS, R., CEULEMANS, H., STALMANS, W. & STEFAN, C. (2000). Nucleotide pyrophosphatases/phosphodiesterases on the move. *Crit. Rev. Biochem. Mol. Biol.,* **35,** 393–432.

BUCKLEY, K.A., GOLDING, S.L., RICE, J.M., DILLON, J.P. & GALLAGHER, J.A. (2003). Release and interconversion of P2 receptor agonists by human osteoblast-like cells. *FASEB J.,* **17,** 1401–1410.

BUXTON, I.L., KAISER, R.A., OXHORN, B.C. & CHEEK, D.J. (2001). Evidence supporting the nucleotide axis hypothesis: ATP release and metabolism by coronary endothelium. *Am. J. Physiol. Heart Circ. Physiol.,* **281,** H1657–H1666.

CHEN, B.C., LEE, C.M. & LIN, W.W. (1996). Inhibition of ecto-ATPase by PPADS, suramin and reactive blue in endothelial cells, C6 glioma cells and RAW 264.7 macrophages. *Br. J. Pharmacol.,* **119,** 1628–1634.

CHEN, B.C. & LIN, W.W. (1997). Inhibition of ecto-ATPase by the P2 purinoceptor agonists, ATPgammaS, alpha,beta-methylene-ATP, and AMP-PNP, in endothelial cells. *Biochem. Biophys. Res. Commun.,* **233,** 442–446.

CONNOLLY, G.P. & DULEY, J.A. (2000). Ecto-nucleotidase of cultured rat superior cervical ganglia: dipyridamole is a novel inhibitor. *Eur. J. Pharmacol.,* **397,** 271–277.

CRACK, B.E., POLLARD, C.E., BEUKERS, M.W., ROBERTS, S.M., HUNT, S.F., INGALL, A.H., MCKECHNIE, K.C., IJZERMAN, A.P. & LEFF, P. (1995). Pharmacological and biochemical analysis of FPL 67156, a novel, selective inhibitor of ecto-ATPase. *Br. J. Pharmacol.,* **114,** 475–481.

DOWD, F.J., LI, L.S. & ZENG, W. (1999). Inhibition of rat parotid ecto-ATPase activity. *Arch. Oral Biol.,* **44,** 1055–1062.

DUNN, P.M. (2000). Fertility: purinergic receptors and the male contraceptive pill. *Curr. Biol.,* **10,** R305–R307.

FORD, S.R., CHENAULT, K.H., BUNTON, L.S., HAMPTON, G.J., MCCARTHY, J., HALL, M.S., PANGBURN, S.J., BUCK, L.M. & LEACH, F.R. (1996). Use of firefly luciferase for ATP measurement: other nucleotides enhance turnover. *J. Biolumin. Chemilumin.,* **11,** 149–167.

FOSTER, C.J., PROSSER, D.M., AGANS, J.M., ZHAI, Y., SMITH, M.D., LACHOWICZ, J.E., ZHANG, F.L., GUSTAFSON, E., MONSMA JR, F.J., WIEKOWSKI, M.T., ABBONDANZO, S.J., COOK, D.N., BAYNE, M.L., LIRA, S.A. & CHINTALA, M.S. (2001). Molecular identification and characterization of the platelet ADP receptor targeted by thienopyridine antithrombotic drugs. *J. Clin. Invest.,* **107,** 1591–1598.

GACHET, C. (2001). Identification, characterization, and inhibition of the platelet ADP receptors. *Int. J. Hematol.,* **74,** 375–381.

GENDRON, F.P., BENREZZAK, O., KRUGH, B.W., KONG, Q., WEISMAN, G.A. & BEAUDOIN, A.R. (2002). Purine signaling and potential new therapeutic approach: possible outcomes of NTPDase inhibition. *Curr. Drug Targets,* **3,** 229–245.

GIJSBERS, R., AOKI, J., ARAI, H. & BOLLEN, M. (2003). The hydrolysis of lysophospholipids and nucleotides by autotaxin (NPP2) involves a single catalytic site. *FEBS Lett.,* **538,** 60–64.

GROBBEN, B., ANCIAUX, K., ROYMANS, D., STEFAN, C., BOLLEN, M., ESMANS, E.L. & SLEGERS, H. (1999). An ecto-nucleotide pyrophosphatase is one of the main enzymes involved in the extracellular metabolism of ATP in rat C6 glioma. *J. Neurochem.,* **72,** 826–834.

HEINE, P., BRAUN, N., HEILBRONN, A. & ZIMMERMANN, H. (1999). Functional characterization of rat ecto-ATPase and ecto-ATP diphosphohydrolase after heterologous expression in CHO cells. *Eur. J. Biochem.,* **262,** 102–107.

JACOBSON, K.A., JARVIS, M.F. & WILLIAMS, M. (2002). Purine and pyrimidine (P2) receptors as drug targets. *J. Med. Chem.,* **45,** 4057–4093.

JOSEPH, S.M., BUCHAKJIAN, M.R. & DUBYAK, G.R. (2003). Colocalization of ATP release sites and ecto-ATPase activity at the extracellular surface of human astrocytes. *J. Biol. Chem.,* **278,** 23331–23342.

KAISER, R.A., OXHORN, B.C., ANDREWS, G. & BUXTON, I.L. (2002). Functional compartmentation of endothelial P2Y receptor signaling. *Circ. Res.,* **91,** 292–299.

KOZIAK, K., KACZMAREK, E., KITTEL, A., SEVIGNY, J., BLUSZTAJN, J.K., SCHULTE AM ESCH II, J., IMAI, M., GUCKELBERGER, O., GOEPFERT, C., QAWI, I. & ROBSON, S.C. (2000). Palmitoylation targets CD39/endothelial ATP diphosphohydrolase to caveolae. *J. Biol. Chem.,* **275,** 2057–2062.

LABASI, J.M., PETRUSHOVA, N., DONOVAN, C., MCCURDY, S., LIRA, P., PAYETTE, M.M., BRISSETTE, W., WICKS, J.R., AUDOLY, L. & GABEL, C.A. (2002). Absence of the P2X7 receptor alters leukocyte function and attenuates an inflammatory response. *J. Immunol.,* **168,** 6436–6445.

LACOMBE, M.L., MILON, L., MUNIER, A., MEHUS, J.G. & LAMBETH, D.O. (2000). The human Nm23/nucleoside diphosphate kinases. *J. Bioenerg. Biomembr.,* **32,** 247–258.

LASLEY, R.D., NARAYAN, P., UITTENBOGAARD, A. & SMART, E.J. (2000). Activated cardiac adenosine A(1) receptors translocate out of caveolae. *J. Biol. Chem.,* **275,** 4417–4421.

LAZAROWSKI, E.R., BOUCHER, R.C. & HARDEN, T.K. (2000). Constitutive release of ATP and evidence for major contribution of ecto-nucleotide pyrophosphatase and nucleoside diphosphokinase to extracellular nucleotide concentrations. *J. Biol. Chem.,* **275,** 31061–31068.

LAZAROWSKI, E.R., BOUCHER, R.C. & HARDEN, T.K. (2003a). Mechanisms of release of nucleotides and integration of their action as P2X- and P2Y-receptor activating molecules. *Mol. Pharmacol.,* **64,** 785–795.

LAZAROWSKI, E.R., HOMOLYA, L., BOUCHER, R.C. & HARDEN, T.K. (1997). Identification of an ecto-nucleoside diphosphokinase and its contribution to interconversion of P2 receptor agonists. *J. Biol. Chem.,* **272,** 20402–20407.

LAZAROWSKI, E.R., SHEA, D.A., BOUCHER, R.C. & HARDEN, T.K. (2003b). Release of cellular UDP-glucose as a potential extracellular signaling molecule. *Mol. Pharmacol.,* **63,** 1190–1197.

MATSUOKA, I., OHKUBO, S., KIMURA, J. & UEZONO, Y. (2002). Adenine nucleotide-induced activation of adenosine A(2B) receptors expressed in *Xenopus laevis* oocytes: involvement of a rapid and localized adenosine formation by ectonucleotidases. *Mol. Pharmacol.,* **61,** 606–613.

MIHAYLOVA-TODOROVA, S.T., TODOROV, L.D. & WESTFALL, D.P. (2002). Enzyme kinetics and pharmacological characterization of nucleotidases released from the guinea-pig isolated vas deferens during nerve stimulation: evidence for a soluble ecto-nucleoside triphosphate diphosphohydrolase-like ATPase and a soluble ecto-5′-nucleotidase-like AMPase. *J. Pharmacol. Exp. Ther.,* **302,** 992–1001.

NEWMAN, E.A. (2003). Glial cell inhibition of neurons by release of ATP. *J. Neurosci.,* **23,** 1659–1666.

NORTH, R.A. (2002). Molecular physiology of P2X receptors. *Physiol. Rev.,* **82,** 1013–1067.

OHKUBO, S., KUMAZAWA, K., SAGAWA, K., KIMURA, J. & MATSUOKA, I. (2001). Beta,gamma-methylene ATP-induced cAMP formation in C6Bu-1 cells: involvement of local metabolism and subsequent stimulation of adenosine A2B receptor. *J. Neurochem.,* **76,** 872–880.

PICHER, M. & BOUCHER, R.C. (2003). Human airway ecto-adenylate kinase: a mechanism to propagate ATP signaling on airway surfaces. *J. Biol. Chem.,* **278,** 11256–11264.

PICHER, M., SEVIGNY, J., D'ORLEANS-JUSTE, P. & BEAUDOIN, A.R. (1996). Hydrolysis of P2-purinoceptor agonists by a purified ectonucleotidase from the bovine aorta, the ATP-diphosphohydrolase. *Biochem. Pharmacol.,* **51,** 1453–1460.

RALEVIC, V. & BURNSTOCK, G. (1998). Receptors for purines and pyrimidines. *Pharmacol. Rev.,* **50,** 413–492.

ROBAYE, B., GHANEM, E., WILKIN, F., FOKAN, D., VAN DRIESSCHE, W., SCHURMANS, S., BOEYNAEMS, J.M. & BEAUWENS, R. (2003). Loss of nucleotide regulation of epithelial chloride transport in the jejunum of P2Y4-null mice. *Mol. Pharmacol.,* **63,** 777–783.

SCHAFER, H.J., SCHEURICH, P., RATHGEBER, G. & DOSE, K. (1978). Synthesis and properties of 8-azido-1, N6-etheno adenosine triphosphate – a fluorescent and photosensitive ATP analog. *Nucleic. Acids. Res.,* **5,** 1345–1351.

SNEDDON, P., WESTFALL, T.D., TODOROV, L.D., TODOROVA, S.M., WESTFALL, D.P., NICKEL, P. & KENNEDY, C. (2000). The effect of P2 receptor antagonists and ATPase inhibition on sympathetic purinergic neurotransmission in the guinea-pig isolated vas deferens. *Br. J. Pharmacol.,* **129,** 1089–1094.

SPELTA, V., MEKHALFIA, A., REJMAN, D., THOMPSON, M., BLACKBURN, G.M. & NORTH, R.A. (2003). ATP analogues with modified phosphate chains and their selectivity for rat P2X2 and P2X2/3 receptors. *Br. J. Pharmacol.,* **140,** 1027–1034.

UMEZU-GOTO, M., KISHI, Y., TAIRA, A., HAMA, K., DOHMAE, N., TAKIO, K., YAMORI, T., MILLS, G.B., INOUE, K., AOKI, J. & ARAI, H. (2002). Autotaxin has lysophospholipase D activity leading to tumor cell growth and motility by lysophosphatidic acid production. *J. Cell Biol.,* **158,** 227–233.

VLASKOVSKA, M., KASAKOV, L., RONG, W., BODIN, P., BARDINI, M., COCKAYNE, D.A., FORD, A.P. & BURNSTOCK, G. (2001). P2X3 knock-out mice reveal a major sensory role for urothelially released ATP. *J. Neurosci.,* **21,** 5670–5677.

VOLLMAYER, P., KOCH, M., BRAUN, N., HEINE, P., SERVOS, J., ISRAR, E., KEGEL, B. & ZIMMERMANN, H. (2001). Multiple ecto-nucleotidases in PC12 cells: identification and cellular distribution after heterologous expression. *J. Neurochem.,* **78,** 1019–1028.

WILLEMS, R., SLEGERS, H., RODRIGUS, I., MOULIJN, A.C., LENJOU, M., NIJS, G., BERNEMAN, Z.N. & VAN BOCKSTAELE, D.R. (2002). Extracellular nucleoside diphosphate kinase NM23/NDPK modulates normal hematopoietic differentiation. *Exp. Hematol.,* **30,** 640–648.

YEGUTKIN, G.G. & BURNSTOCK, G. (2000). Inhibitory effects of some purinergic agents on ecto-ATPase activity and pattern of stepwise ATP hydrolysis in rat liver plasma membranes. *Biochim. Biophys. Acta.,* **1466,** 234–244.

YEGUTKIN, G.G., HENTTINEN, T. & JALKANEN, S. (2001). Extracellular ATP formation on vascular endothelial cells is mediated by ecto-nucleotide kinase activities *via* phosphotransfer reactions. *FASEB J.,* **15,** 251–260.

YEGUTKIN, G.G., HENTTINEN, T., SAMBURSKI, S.S., SPYCHALA, J. & JALKANEN, S. (2002). The evidence for two opposite, ATP-generating and ATP-consuming, extracellular pathways on endothelial and lymphoid cells. *Biochem. J.,* **367,** 121–128.

ZIMMERMANN, H. (2000). Extracellular metabolism of ATP and other nucleotides. *Naunyn Schmiedebergs Arch. Pharmacol.,* **362,** 299–309.

(Received March 9, 2004
Revised April 10, 2004
Accepted May 6, 2004)